Available online at www.sciencedirect.com
ScienceDirect
Journal of Solid State Chemistry 180 (2007) 2635–2640
JOURNAL OF SOLID STATE CHEMISTRY
www.elsevier.com/locate/jssc

Rapid Communication

Synthesis, characterization and activity of alumina-supported cobalt nitride for NO decomposition

Zhiwei Yao[a], Aimin Zhu[a,b], Jing Chen[a], Xinkui Wang[a], C.T. Au[c], Chuan Shi[a,*]

[a]Laboratory of Plasma Physical Chemistry, Dalian University of Technology, Dalian 116024, China
[b]State Key Laboratory of Material Modification by Ion, Electron and Laser Beams, Dalian University of Technology, Dalian 116024, China
[c]Department of Chemistry, Center for Surface Analysis and Research, Hong Kong Baptist University, Kowloon Tong, Hong Kong

Received 22 January 2007; received in revised form 30 May 2007; accepted 4 June 2007
Available online 21 July 2007

Abstract

A new type of transition metal nitride, viz. alumina-supported cobalt nitride, was synthesized for the first time by NH_3-temperature-programmed reaction, and its structure was characterized by BET, X-ray diffraction (XRD) and X-ray photoelectron spectroscopic (XPS) techniques. The supported cobalt nitride performs much better than its bulk counterpart for NO decomposition, owing to its small crystal size, high thermal stability and big surface area.

Keywords: Alumina-supported cobalt nitride; Thermal stability; NO decomposition

1. Introduction

Due to the fact that transition metal nitrides possess chemical properties similar to those of noble metals, they have received much attention. Various kinds of transition metal nitrides such as monometallic VN, Mo_2N, W_2N [1–3], and bimetallic such as Co_3Mo_3N, Ni_2Mo_3N, Fe_3Mo_3N [4], as well as supported nitrides Mo_2N/γ-Al_2O_3, Co_3Mo_3N/γ-Al_2O_3 and Ni_2Mo_3N/γ-Al_2O_3 [5,6] have been synthesized. The application of these materials has been found in catalytic reactions such as NH_3 synthesis [7], NO removal [8–12], hydrogenation (HYN), hydrodesulfurization (HDS), hydrodenitrogenation (HDN) and hydrodeoxygenation (HDO) [13]. Compared to the nitrides of Group V–VI metals (e.g., V, Mo and W), the nitrides of Fe, Co and Re (Group VII–VIII) have received far less attention due to their poor thermal stability [14]. The results of earlier observation indicated that Co_4N was unstable and undergoing a stepwise decomposition with N_2 evolution below 700 °C: $Co_4N \rightarrow Co_3N + Co$, $Co_3N \rightarrow Co_2N + Co$, $Co_2N \rightarrow CoN + Co$ [15]. Kojima and Aika reported the use of Re_3N as catalysts for ammonia synthesis at 623 K under 0.1 MPa. Although activity was high at the initial stage, there was deactivation due to Re_3N decomposition [16]. For the utilization of nitrides of Group VII–VIII transition metals, a means of enhancing the thermal stability remains as a meaningful challenge in the field.

In this study, the supported cobalt nitride catalyst was synthesized according to the following strategy: (i) to enlarge the surface area of the catalyst by dispersing cobalt nitride on γ-Al_2O_3, (ii) to generate nanosized cobalt nitride particles, and (iii) to enhance the thermal stability of cobalt nitride by the interaction with γ-Al_2O_3. The reaction of NO direct decomposition was selected as a probe to study the catalytic properties of the alumina-supported cobalt nitride material.

2. Experimental

The Co_3O_4/γ-Al_2O_3 precursor with Co loading of 30 wt% was prepared by method of wetness incipient impregnation via stirring γ-Al_2O_3 ($S_{BET} \approx 250\,m^2/g$, 40–60 mesh) in an aqueous cobalt nitrate ($Co(NO_3)_2 \cdot 6H_2O$) solution, followed by drying at 120 °C for 12 h and calcination at 500 °C for 3 h. The bulk cobalt nitride and

*Corresponding author.
E-mail address: chuanshi@dlut.edu.cn (C. Shi).

0022-4596/$ - see front matter © 2007 Published by Elsevier Inc.
doi:10.1016/j.jssc.2007.06.031

γ-Al_2O_3 supported cobalt nitride catalysts were generated by means of NH_3-temperature-programmed reaction. Typically, about 2.0 g of the oxide precursor was placed in a microreactor and a flow of NH_3 (150 ml/min) was introduced into the system. Initially, the sample was linearly heated from room temperature (RT) to 300 °C over a period of 30 min, followed by a rise in temperature from 300 to 450 °C at a rate of 0.67 °C/min, and a further increase from 450 to 700 °C at a rate of 1.67 °C/min. The temperature was kept at 700 °C for 2 h before cooling to RT in a NH_3 flow. The material was then purged with N_2 for 10 min followed by passivation in 1% O_2/99% N_2 for 12 h. The cobalt metal and γ-Al_2O_3 supported cobalt metal catalysts were prepared from their corresponding oxide precursors using H_2 at 700 °C for 2 h. The material was also passivated in 1% O_2/99% N_2 for 12 h before it was exposed to air.

The BET surface areas of the passivated samples were measured on an ASAP 2010 instrument. The N_2 gas was adopted for standard five-point BET surface area measurements. X-ray diffraction (XRD) examination was performed using an X-ray diffractometer (Rigaku D-Max Rotaflex) with Cu$K\alpha$ radiation ($\lambda = 1.5404$ Å). The particle size was estimated according to the Scherrer formula. The temperature-programmed decomposition of the as-prepared nitrides was examined on a flow system equipped with a mass spectrometer (MS, HP G1800A). X-ray photoelectron spectroscopic (XPS) investigation was conducted using an Al$K\alpha$ source operated at 10 kV and 15 mA (Leybold Heraeus-Shengyang SKL-12 with VG CLAM 4 MCD analyzer); charging effects were corrected by means of adventitious carbon (284.6 eV) referencing.

The catalytic activity was evaluated using a quartz microreactor (i.d. 4 mm). The temperature was measured with a thermocouple placed adjacent to the catalyst outside the reactor. A reaction gas mixture composed of 1000 ppm NO and He as balance was fed through the catalyst (0.4 g) which had been pretreated in pure He at 400 °C for 1 h. The effluent gases were monitored by means of online GC with a TCD detector. A molecular sieve 5A column was used to separate H_2, O_2, N_2 and NO. The amount of N_2 produced was used to calculate the conversion of NO to N_2.

3. Results and discussion

Table 1 summarizes the phase, specific surface area and crystal size of bulk and alumina-supported cobalt nitride samples prepared by ammonolysis of the corresponding oxide precursors. It can be observed that significantly higher surface area is obtained for the alumina-supported cobalt nitride compared with that of Co_4N. The surface area of the sample is in reasonable agreement with that estimated from the average crystal size.

Fig. 1 shows the XRD patterns of bulk Co_4N and Co_4N/γ-Al_2O_3, as well as those of Co metal and γ-Al_2O_3, respectively. The XRD patterns of bulk Co_4N and Co_4N/γ-Al_2O_3 are consistent with those reported in the literature for pure Co_4N [17]. Nevertheless, compared to those of pure γ-Al_2O_3 the peaks of γ-Al_2O_3 in Co_4N/γ-Al_2O_3 shift to lower 2θ angle. It indicates that there is significant interaction between Co_4N and γ-Al_2O_3. Fang et al. reported that the grain structure of Co_4N is similar to that of Co, which might easily lead to misinterpretation [15]. We also found that it is impossible to differentiate Co_4N from Co because the XRD pattern of Co_3O_4 reduced in H_2 at 700 °C for 2 h looks exactly the same as that of Co_4N (Fig. 1).

In order to confirm the formation of Co_4N during Co_3O_4 nitridation, temperature-programmed decomposition experiments were conducted. There are clear discrepancies between the decomposition profiles of Co_4N and Co_4N/γ-Al_2O_3 as shown in Fig. 2. Over the Co_4N sample, we detected an intense N_2 peak at 620 °C and there was no obvious desorption of NH_3 and H_2O in the entire temperature range adopted for the study; this is a clear indication that the N_2 originated from the decomposition of Co_4N. In the case of Co_4N/γ-Al_2O_3, the N_2 peak was at 420 °C and there was desorption of NH_3 and H_2O within the 200–600 °C range. The former was strong whereas the

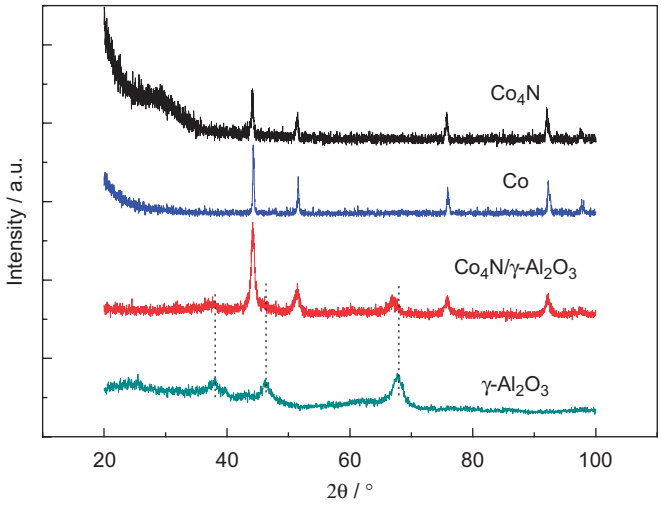

Fig. 1. XRD patterns of Co_4N, Co, Co_4N/γ-Al_2O_3 and γ-Al_2O_3.

Table 1
Phase, BET surface areas and crystal size of catalysts

Metal oxide precursor	Phase identified after being nitrided in NH_3	Surface area of nitride ($m^2 g^{-1}$)	Crystal size of the nitrided phase (nm)
Co_3O_4	Co_4N	1.3	25
Co_3O_4/γ-Al_2O_3	Co_4N/γ-Al_2O_3	148.4	14

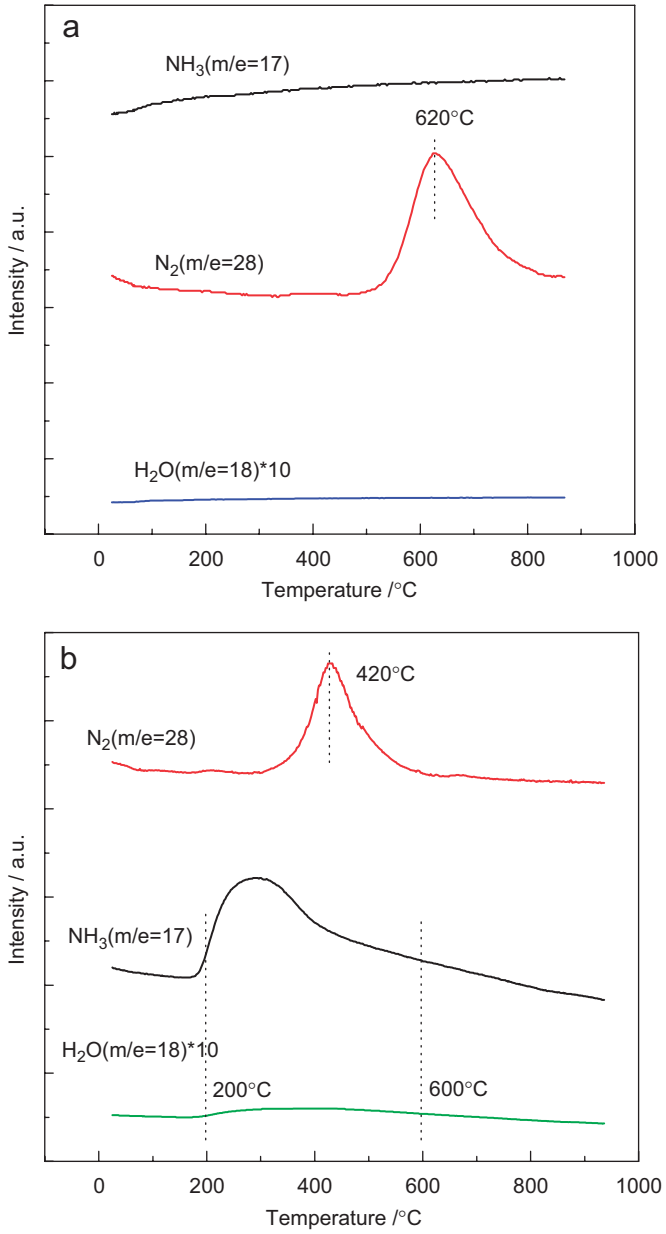

Fig. 2. Temperature-programmed decomposition profiles of (a) Co_4N and (b) Co_4N/γ-Al_2O_3 samples.

latter was weak. According to the work of Nagai et al. [18], there was the formation of NH_x ($x = 1, 2, 3$) species on the surface of supported nitride catalyst during cooling to RT under NH_3 after nitridation, and the adsorbed NH_x ($x = 1, 2, 3$) decomposed via sequential dehydrogenation, giving ultimately N_2 and H_2. Thus, it is reasonable to deduce that there were weakly and strongly adsorbed NH_x ($x = 1, 2, 3$) species on Co_4N/γ-Al_2O_3 and the weakly adsorbed NH_x ($x = 1, 2, 3$) desorbed as NH_3 (g). It is not possible to be confirmative whether the N_2 peak at 420 °C is due to decomposition of Co_4N or dissociation of strongly adsorbed NH_x ($x = 1, 2, 3$). The hydrogen originated from NH_x ($x = 1, 2, 3$) decomposition desorbed as H_2 (g) or reacted with surface oxygen to give water. We could not monitor H_2 desorption because the MS equipment was not designed for hydrogen detection. Nonetheless, the detection of the weak H_2O desorption signal suggests that there was only a small amount of oxygen on the surface of Co_4N/γ-Al_2O_3 and there was NH_x ($x = 1, 2, 3$) dissociation. In addition, our NH_3-TPD results (not shown) on Co_4N/γ-Al_2O_3 revealed that the temperature (480 °C) for N_2 desorption in NH_3-TPD investigation is close to that detected in temperature-programmed decomposition reaction (Fig. 2(b)). If one could accept that the N_2 peak at 420 °C originated from NH_x ($x = 1, 2, 3$), the Co_4N formed on γ-Al_2O_3 should be thermally stable and have kept its structure reasonably well up to a temperature as high as 950 °C.

The XPS Co 2*p* spectra of Co_4N and Co_4N/γ-Al_2O_3 as well as that of Co metal are shown in Fig. 3. The relative intensities of spin–orbit doublet peaks are given by the ratio of their respective degeneracy, and the $I(2p_{3/2})/I(2p_{1/2})$ intensity ratio for the $Co(2p_{3/2})/Co(2p_{1/2})$ doublet is 2/1. A splitting energy of 15.2 eV is expected for the doublet. By means of curve fitting, the cobalt oxidation states and the corresponding distribution of cobalt species are estimated (Table 2). As shown in Fig. 3(a), the binding energies of Co $2p_{1/2}$ and Co $2p_{3/2}$ for Co_4N are 796.3 and 781.1 eV, respectively. The value of Co $2p_{3/2}$ is consistent with that reported by Milad et al. [17]. The value is higher than that of Co^{2+} (779.9 ± 0.4 eV) but slightly lower than that of Co^{3+} (781.6 ± 0.3 eV) [19]. Accordingly, we denote the Co species of Co_4N as $Co^{\delta+}$, where $2 < \delta < 3$. For a Co sample obtained via H_2-treating a cobalt oxide sample after passivation, there are two states of surface Co. The peaks at binding energy of 777.9 and 793.1 eV are assigned to Co^0, and those at 780.5 and 795.7 eV, to Co_3O_4 (Fig. 3(d)) [20]. The results of XPS investigation indicated that of metal cobalt and cobalt oxide coexist on the H_2-reduced cobalt oxide sample. As for the passivated Co_4N/γ-Al_2O_3 sample (Fig. 3(b)), the peaks at binding energy of 781.6 and 796.8 eV are closer to those of Co_4N (781.1 and 796.3 eV) in comparison to that of Co^0 (778.0 and 793.0 eV) [20]. The results indicated that the cobalt oxide precursor on γ-Al_2O_3 was converted to Co_4N but not Co^0 during the ammonolysis process. In view of point that N_2 peak shown in Fig. 2(b) could be a result of Co_4N decomposition, a portion of the Co_4N/γ-Al_2O_3 sample was pretreated in a flow of He at 500 °C for 3 h to eliminate surface NH_x ($x = 1, 2, 3$). The Co 2*p* spectrum of the treated sample (Fig. 3(c)) is similar to that of the un-treated one (Fig. 3(b)). The results inferred that there was Co_4N on γ-Al_2O_3 after the N_2 desorption at 420 °C (Fig. 2(b)). In other words, the evolution of N_2 originated from NH_x ($x = 1, 2, 3$) decomposition rather than from thermal decomposition of Co_4N.

The catalytic activity of Co_4N and Co_4N/γ-Al_2O_3 catalysts for NO decomposition are shown in Fig. 4. It can be observed that the effective temperature range for NO decomposition is 200–450 °C for Co_4N and 100–700 °C for Co_4N/γ-Al_2O_3. In the cases of Cu-ZSM-5 and Pd/Al_2O_3, the effective temperatures for high NO decomposition

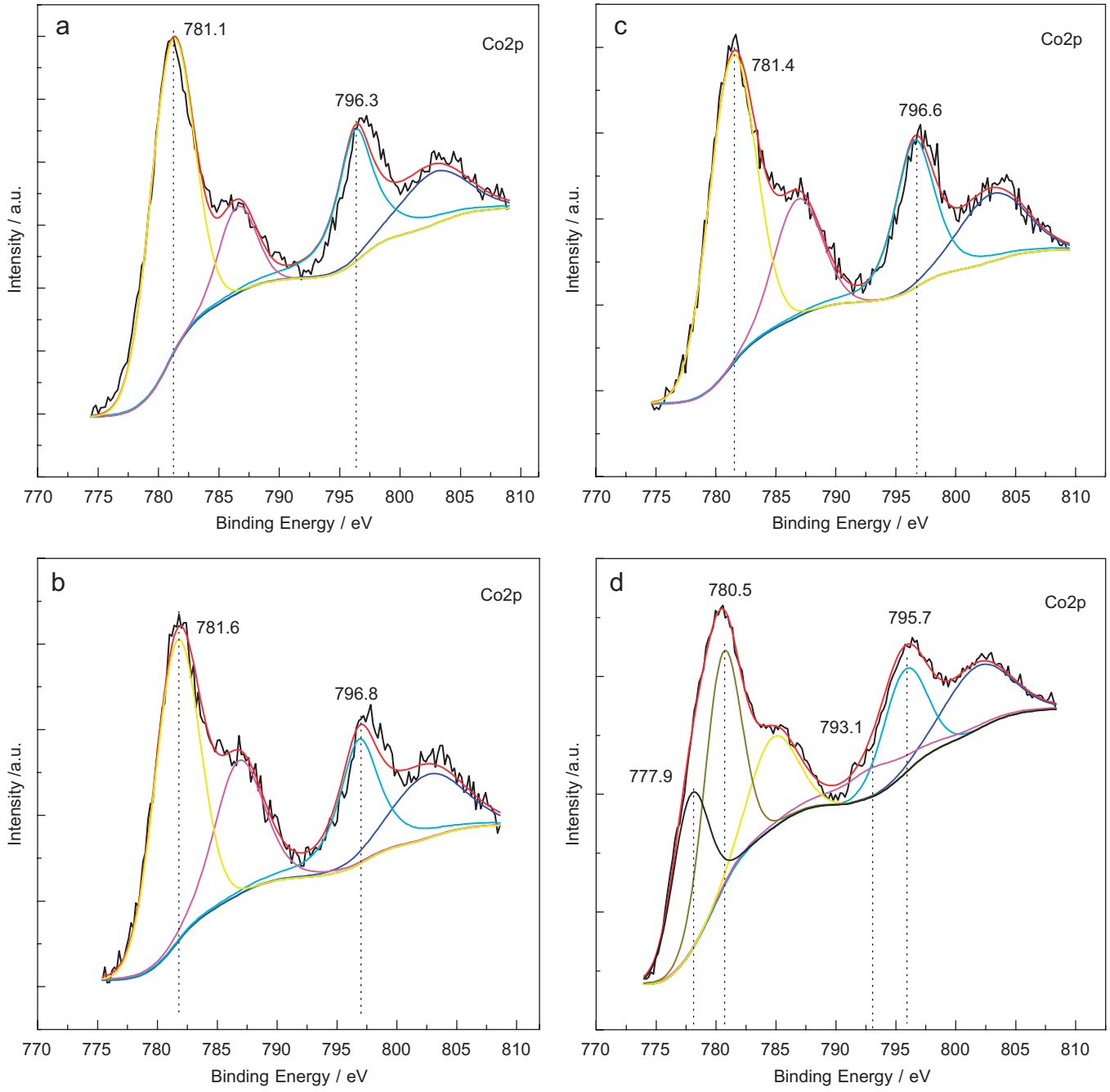

Fig. 3. Co 2*p* spectra of (a) Co_4N, (b) Co_4N/γ-Al_2O_3, (c) Co_4N/γ-Al_2O_3 (treated in He at 500 °C for 3 h) and (d) Co in XPS study.

Table 2
XPS parameters derived from curve-fitting the Co $2p_{3/2}$ envelope

Catalyst	Co^{2+} or Co^{3+} B.E. (eV)	$Co^{\delta+}$ $(2<\delta<3)$ B.E. (eV)	Co^{o} B.E. (eV)
Co_4N		781.1	
Co_4N/γ-Al_2O_3		781.6	
Co_4N/γ-Al_2O_3 (500 °C pretreated)		781.4	
Co	780.5		777.9

were 400–550 °C and above 500 °C, respectively, as reported by Haneda et al. [21]. Compared to Cu-ZSM-5 and Pd/Al_2O_3, the bulk and supported cobalt nitride catalysts of the present study showed a wider temperature window and a lower temperature of initial activity for NO decomposition, and the Co_4N/γ-Al_2O_3 catalyst was of higher catalyst activity, than the Co_4N within the temperature range of 100–250 °C. In addition, at temperature higher than 450 °C, the Co_4N/γ-Al_2O_3 catalyst remained active and stable while the Co_4N catalyst started

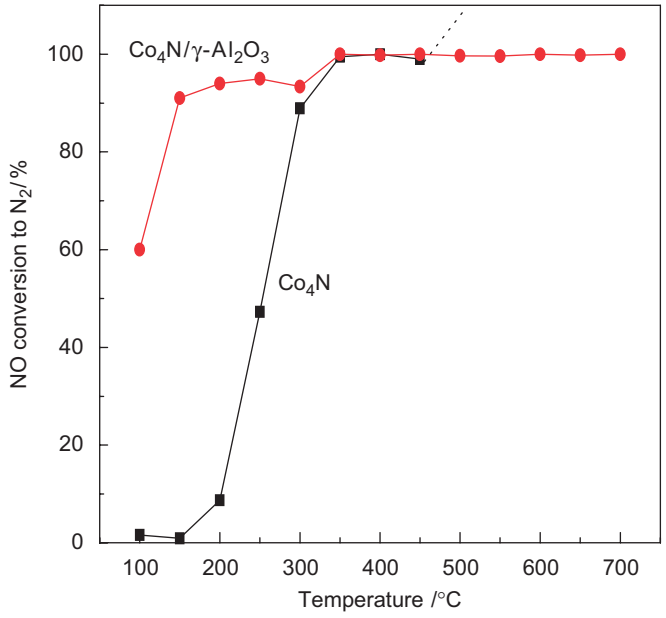

Fig. 4. Variation of NO conversion to N_2 as a function of reaction temperature over Co_4N and Co_4N/γ-Al_2O_3 catalysts. Reaction conditions: NO = 1000 ppm, gas flow rate = 20 cm^3/min, $W/F = 1.2$ g/scm^3.

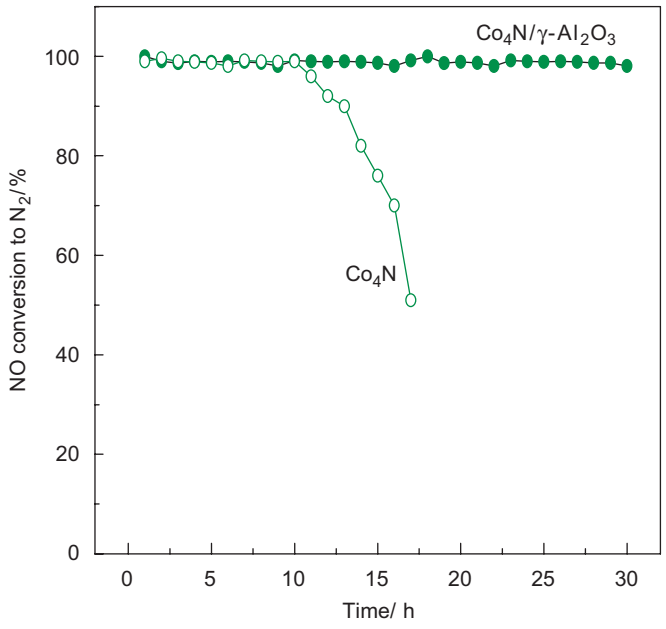

Fig. 5. Time dependence of NO decomposition to N_2 over Co_4N and Co_4N/γ-Al_2O_3 catalysts at 400 °C (reaction conditions: same as those of Fig. 4).

to decompose with the evolution of N_2 (dashed line in Fig. 4). The stability of Co_4N and Co_4N/γ-Al_2O_3 catalysts for NO decomposition are shown in Fig. 5. It can be observed that the Co_4N catalyst showed an initial activity of ca. 100% but deactivated after 10 h of on-stream reaction: NO conversion to N_2 decreased from ca. 100% to ca. 51% within a period of 17 h. As for the Co_4N/γ-Al_2O_3 catalyst, NO conversion to N_2 stayed at ca. 100% throughout the entire test period of 30 h. Taking the results

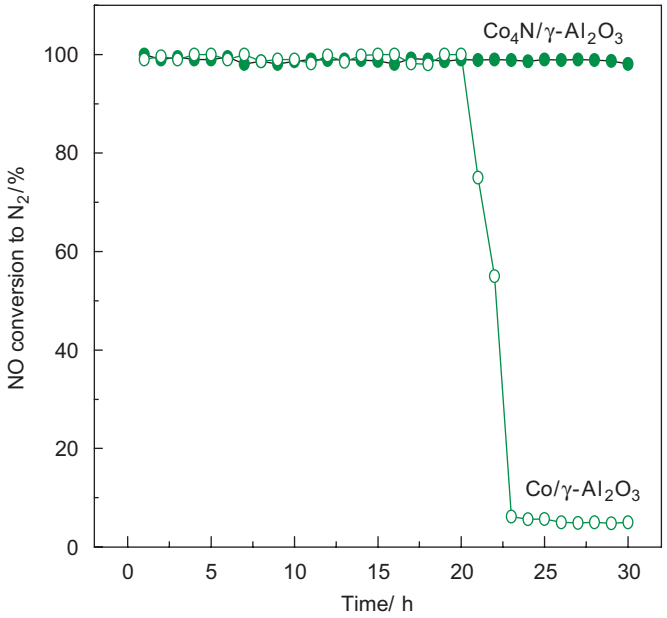

Fig. 6. Time dependence of NO decomposition to N_2 over Co_4N/γ-Al_2O_3 and Co/γ-Al_2O_3 catalysts at 600 °C (reaction conditions: same as those of Fig. 4).

of Table 1 into account, the activity of the two cobalt nitride catalysts can be related to their surface area and particle size. The thermal stability of cobalt nitride is enhanced by having the nanoparticles dispersed on γ-Al_2O_3, and according to the XRD results, the dispersed particles are stabilized via strong interaction between Co_4N and γ-Al_2O_3. Fig. 6 shows the time dependence of NO conversion to N_2 over Co_4N/γ-Al_2O_3 and Co/γ-Al_2O_3 at 600 °C. It can be seen that NO conversion was ca. 100% throughout the entire period of 30 h over Co_4N/γ-Al_2O_3. It is a clear indication that the alumina-supported cobalt nitride is thermally and catalytically stable for NO removal. Over Co/γ-Al_2O_3, although a high NO conversion of ca. 100% was attained, fast deactivation occurred after 20 h of on-stream time. As reported by Xiao et al. [22], heavy accumulation of surface oxygen on well-dispersed Co caused the deactivation of catalyst in NO decomposition. We take that the significant difference in activity observed over the two samples is another piece of evidence to show that the Co_4N/γ-Al_2O_3 synthesized is indeed Co_4N/γ-Al_2O_3 rather than Co/γ-Al_2O_3.

4. Conclusions

In conclusion, despite it is not possible to confirm by means of XRD investigation whether cobalt oxide converted to Co_4N or reduced to Co metal in the ammonolysis process, the results of XPS and temperature-programmed decomposition investigation over bulk Co_4N and Co_4N/γ-Al_2O_3 provide proofs of the formation of Co_4N on γ-Al_2O_3 after the nitridation of the Co_3O_4/γ-Al_2O_3 precursor. Furthermore, the significant difference in activity between Co_4N/γ-Al_2O_3 and Co/γ-Al_2O_3 provided

supplementary evidence that the Co_4N/γ-Al_2O_3 synthesized is indeed Co_4N/γ-Al_2O_3. It was observed that due to the nanosize and good dispersion, the supported Co_4N exhibits thermal stability and surface area significantly higher than that of bulk Co_4N. As a consequence, the former showed much better activity and stability for NO decomposition in the temperature range 100–700 °C. It was noteworthy that Co_4N particles can also be stabilized by having them dispersed on other supporters such as HZSM-5, SiO_2, CeO_2 and so on. Comprehensive studies for the interaction between metal nitrides and support materials might provide new insights that could lead to enhanced thermal stability of nitrides of Group VII–VIII transition metals.

Acknowledgments

The work was supported by the National Natural Science Foundation of China (No. 20573014) and the Natural Science Foundation of Liao-ning Province (20041072).

References

[1] H. Kwon, S. Choi, L.T. Thompson, J. Catal. 184 (1999) 236–246.
[2] J.-G. Choi, R.L. Curl, L.T. Thompson, J. Catal. 146 (1994) 218–227.
[3] J.H. Kim, K.L. Kim, Appl. Catal. A 181 (1999) 103–111.
[4] S. Alconchel, F. Sapina, D. Beltran, A. Beltran, J. Mater. Chem. 8 (1998) 1901–1909.
[5] M. Nagai, Y. Goto, A. Irisawa, S. Omi, J. Catal. 191 (2000) 128.
[6] S. Korlann, B. Diaz, M.E. Bussell, Chem. Mater. 14 (2002) 4049–4058.
[7] C.J.H. Jacobsen, Chem. Commun. (2000) 1057–1058.
[8] H. He, H.X. Dai, K.Y. Ngan, C.T. Au, Catal. Lett. 71 (2001) 147–153.
[9] C. Shi, X.F. Yang, A.M. Zhu, C.T. Au, Catal. Today 93–95 (2004) 819–826.
[10] C. Shi, A.M. Zhu, X.F. Yang, C.T. Au, Appl. Catal. A 276 (2004) 223–230.
[11] C. Shi, X.F. Yang, A.M. Zhu, C.T. Au, Catal. Lett. 97 (2004) 9–16.
[12] C. Shi, A.M. Zhu, X.F. Yang, C.T. Au, Appl. Catal. A 293 (2005) 83–90.
[13] E. Furimsky, Appl. Catal. A 240 (2003) 1–28.
[14] S.T. Oyama, in: S.T. Oyama (Ed.), The Chemistry of Transition Metal Carbides and Nitrides, Blackie, New York, 1996, p. 1.
[15] J.S. Fang, L.C. Yang, C.S. Hsu, G.S. Chen, Y.W. Lin, G.S. Chen, J. Vac. Sci. Technol. A 22 (2004) 698–704.
[16] R. Kojima, K. Aika, Appl. Catal. A 209 (2001) 317–325.
[17] I.K. Milad, K.J. Smith, P.C. Wong, K.A.R. Mitchell, Catal. Lett. 52 (1998) 113–119.
[18] M. Nagai, Y. Goto, A. Miyoshi, K. Hada, K. Oshikawa, S. Omi, J. Catal. 182 (1999) 292–301.
[19] K. Hada, M. Nagai, S. Omi, J. Phys. Chem. B 105 (2001) 4084–4093.
[20] G. Jacobs, J.A. Chaney, P.M. Patterson, T.K. Das, B.H. Davis, Appl. Catal. A 264 (2004) 203–212.
[21] M. Haneda, Y. Kintaichi, N. Bion, H. Hamada, Appl. Catal. B 46 (2003) 473–482.
[22] Y. Xiao, J. Ma, X.Y. Yang, Chin. J. Catal. 20 (1999) 495–498.